

Eigenstates of Operating Quantum Computer: Hypersensitivity to Static Imperfections

Giuliano Benenti^(a), Giulio Casati^(a,b), Simone Montangero^(a), and Dima L. Shepelyansky^(c)

^(a)*International Center for the Study of Dynamical Systems, Università degli Studi dell'Insubria and Istituto Nazionale per la Fisica della Materia, Unità di Como, Via Valleggio 11, 22100 Como, Italy*

^(b)*Istituto Nazionale di Fisica Nucleare, Sezione di Milano, Via Celoria 16, 20133 Milano, Italy*

^(c)*Laboratoire de Physique Quantique, UMR 5626 du CNRS, Université Paul Sabatier, 31062 Toulouse Cedex 4, France*

(December 21, 2001)

We study the properties of eigenstates of an operating quantum computer which simulates the dynamical evolution in the regime of quantum chaos. Even if the quantum algorithm is polynomial in number of qubits n_q , it is shown that the ideal eigenstates become mixed and strongly modified by static imperfections above a certain threshold which drops *exponentially* with n_q . Above this threshold the quantum eigenstate entropy grows linearly with n_q but the computation remains reliable during a time scale which is polynomial in the imperfection strength and in n_q .

PACS numbers: 03.67.Lx, 05.45.Mt, 24.10.Cn

Feynman suggested that a quantum computer could simulate quantum mechanical systems exponentially faster than a classical computer [1] while Shor significantly extended this class by his ground-breaking algorithm for integer factorization [2]. More recently, a few quantum algorithms which achieve the exponential speedup have been developed for various quantum and classical physical systems, ranging from some many-body problems [3] to spin lattices [4], and models of quantum and classical chaos [5–7]. These algorithms have been constructed for idealized perfect quantum computers. In reality, any laboratory implementation of a quantum computer would involve imperfections [8]. The first investigations have shown a certain stability of quantum evolution and algorithms with respect to decoherence effects [9], noisy gates [10–12], and static imperfections [7,8]. These studies have focused on the fidelity of quantum computation as a function of time during the realization of a given quantum algorithm.

In this Letter, we study the properties of the eigenstates of an operating quantum computer in the presence of static imperfections. The computer is simulating efficiently the time evolution of a dynamical quantum system described by the sawtooth map [7]. We focus on the regime of quantum ergodicity, in which eigenfunctions are given by a complex superposition of a large number of quantum register states. In this regime, the effect of a perturbation is enhanced by a factor which is *exponential* in the number of qubits. This phenomenon has close links with the enormous enhancement of weak interactions in heavy nuclei [13]. In the following we illustrate this general effect for the case of static imperfections in a realistic model of quantum computer hardware.

The classical sawtooth map is given by

$$\bar{n} = n + k(\theta - \pi), \quad \bar{\theta} = \theta + T\bar{n}, \quad (1)$$

where (n, θ) are conjugated action-angle variables ($0 \leq$

$\theta < 2\pi$), and the bars denote the variables after one map step. Introducing the rescaled momentum variable $p = Tn$, one can see that the classical dynamics depends only on the single parameter $K = kT$, so that the motion is stable for $-4 < K < 0$ and completely chaotic for $K < -4$ and $K > 0$. The quantum evolution for one map iteration is described by a unitary operator \hat{U} acting on the wave function ψ :

$$\bar{\psi} = \hat{U}\psi = e^{-iT\hat{n}^2/2} e^{ik(\hat{\theta}-\pi)^2/2} \psi, \quad (2)$$

where $\hat{n} = -i\partial/\partial\theta$ (we set $\hbar = 1$). The classical limit corresponds to $k \rightarrow \infty$, $T \rightarrow 0$, and $K = kT = \text{const}$. In this Letter, we study the quantum sawtooth map (2) in the regime of quantum ergodicity, with $K = \sqrt{2}$, $-\pi \leq p < \pi$ (torus geometry). The classical limit is obtained by increasing the number of qubits $n_q = \log_2 N$ (N number of levels), with $T = 2\pi/N$ ($k = K/T$, $-N/2 \leq n < N/2$). The quantum algorithm [7] simulates with exponential efficiency the quantum dynamics (2) using a register of n_q qubits. It is based on the forward/backward quantum Fourier transform [14] between the θ and n representations and requires $2n_q$ Hadamard gates and $3n_q^2 - n_q$ controlled-phase-shift gates per map iteration [7].

Following [8], we model the quantum computer hardware as an one-dimensional array of qubits (spin halves) with static imperfections, i.e. fluctuations in the individual qubit energies and residual short-range inter-qubit couplings. The model is described by the many-body Hamiltonian

$$\hat{H}_S = \sum_i (\Delta_0 + \delta_i) \hat{\sigma}_i^z + \sum_{i < j} J_{ij} \hat{\sigma}_i^x \hat{\sigma}_j^x, \quad (3)$$

where the $\hat{\sigma}_i$ are the Pauli matrices for the qubit i , and Δ_0 is the average level spacing for one qubit. The second sum in (3) runs over nearest-neighbor qubit pairs, and δ_i , J_{ij} are randomly and uniformly distributed in the intervals $[-\delta/2, \delta/2]$ and $[-J, J]$, respectively. We study

numerically the many-qubit eigenstates of the quantum computer (3) running the quantum algorithm described above. The algorithm is realized by a sequence of instantaneous and perfect one- and two-qubit gates, separated by a time interval τ_g , during which the Hamiltonian (3) gives unwanted phase rotations and qubit couplings. We assume that the average phase accumulation given by Δ_0 can be eliminated, e.g. by means of refocusing techniques [15].

Since the evolution operator (2) remains periodic in the presence of static imperfections, $\hat{U}^{(\epsilon)}(\tau + T) = \hat{U}^{(\epsilon)}(\tau)$ ($\epsilon \equiv \delta\tau_g$), all the informations about the system dynamics are included in the quasienergy eigenvalues $\lambda_\alpha^{(\epsilon)}$ and eigenstates $\phi_\alpha^{(\epsilon)}$ of the Floquet operator:

$$\hat{U}^{(\epsilon)}(T)\phi_\alpha^{(\epsilon)} = \exp(i\lambda_\alpha^{(\epsilon)})\phi_\alpha^{(\epsilon)}. \quad (4)$$

In Fig.1 (top left) we show the parametric dependence of the quasienergy eigenvalues on the dimensionless imperfection strength ϵ , for a given realization of δ_i , at $J = 0$ and for $n_q = 9$ qubits. One can clearly see the presence of avoided crossings, a typical signature of ergodic dynamics. The variation of a given quasienergy eigenstate with ϵ is illustrated by the Husimi functions [16] of Fig.1. At $\epsilon = 0$ the eigenfunctions display a complex pattern delocalized in the phase space (see Fig.1 top right). The symmetries of the Husimi functions ($\theta \rightarrow 2\pi - \theta$, $p \rightarrow -p$) are destroyed when $\epsilon \neq 0$ [17]. The eigenfunctions in the presence of imperfections give a good representation of the unperturbed ($\epsilon = 0$) eigenfunctions of the quantum sawtooth map (2) at most until the first avoided crossing. After that one cannot make a one to one correspondence with the unperturbed case. This is confirmed by the last two Husimi functions of Fig.1, taken for the chosen level in the vicinity of the first avoided crossing (bottom left, $\epsilon = 4 \times 10^{-4}$) and for a stronger imperfection strength (bottom right, $\epsilon = 10^{-3}$). In the first case there is still some similarity with the corresponding Husimi function at $\epsilon = 0$, while in the latter case any resemblance has been effaced.

A more quantitative indication of the similarity between exact and perturbed eigenstates is provided by the quantum eigenstate entropy,

$$S_\alpha = - \sum_{\beta=1}^N p_{\alpha\beta} \log_2 p_{\alpha\beta}, \quad (5)$$

where $p_{\alpha\beta} = |\langle \phi_\beta^{(0)} | \phi_\alpha^{(\epsilon)} \rangle|^2$. In this way $S_\alpha = 0$ if $\phi_\alpha^{(\epsilon)}$ coincides with one eigenstate at $\epsilon = 0$, $S_\alpha = 1$ if $\phi_\alpha^{(\epsilon)}$ is equally composed of two ideal ($\epsilon = 0$) eigenstates, and the maximal value $S_\alpha = n_q$ is obtained if all $\phi_\beta^{(0)}$ ($\beta = 1, \dots, N = 2^{n_q}$) contribute equally to $\phi_\alpha^{(\epsilon)}$. In order to reduce statistical fluctuations, we average S_α over $\alpha = 1, \dots, N$ and over $3 \leq N_D \leq 10^3$ random realizations of δ_i, J_{ij} . In this way the total number of eigenstates is

$N_D N \approx 10^4$. The variation of the average quantum entropy S with ϵ is shown in Fig.2. It demonstrates that S grows from $S = 0$ at $\epsilon = 0$ to a saturation value $S \approx n_q$ corresponding to maximal mixing of unperturbed eigenstates. We study this crossover for $4 \leq n_q \leq 12$ at $J = 0$ and find that the mixing takes place at smaller values when n_q increases. In Fig.3 we show that the critical imperfection strength ϵ_χ at which $S = 1$ drops exponentially with the number of qubits. This exponential dependence holds also in a simple toy model with a single impurity, in which an energy fluctuation δ is switched on for a single qubit and only for one time interval τ_g between two elementary gates (e.g., after the first quantum Fourier transform).

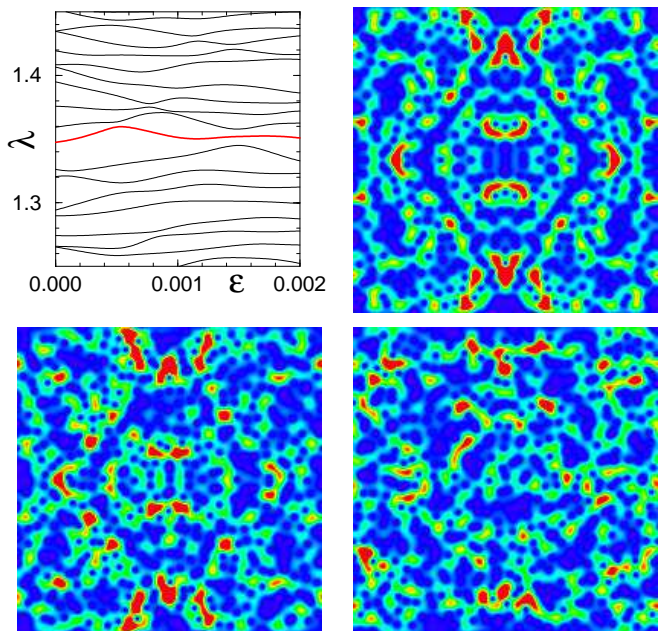


FIG. 1. Parametric dependence of the quasienergy eigenvalues on the imperfection strength ϵ for a given random realization of δ_i , at $J = 0$, $n_q = 9$ (top left); for the red-colored level the corresponding Husimi functions in action-angle variables (p, θ) ($-\pi \leq p < \pi$ -vertical axis- and $0 \leq \theta < 2\pi$ -horizontal axis-) are given at $\epsilon = 0$ (top right), $\epsilon = 4 \times 10^{-4}$ (bottom left), and $\epsilon = 10^{-3}$ (bottom right). We choose the ratio of the action-angle uncertainties $s = \Delta p / \Delta \theta = T \Delta n / \Delta \theta = 1$ ($\Delta p \Delta \theta = T/2$). The color is proportional to the density: blue for zero and red for maximal density.

The exponential drop of the threshold ϵ_χ can be understood following a theory originally developed for the parity breaking induced by weak interaction in the scattering of polarized neutrons on complex nuclei [13]. Indeed, due to quantum chaos in (2), the Floquet problem (4) has ergodic eigenstates, $\phi_\alpha^{(0)} = \sum_{m=1}^N c_\alpha^{(m)} u_m$, with u_m being quantum register states and $c_\alpha^{(m)}$ randomly fluctuating components, with $|c_\alpha^{(m)}| \sim 1/\sqrt{N}$. For the model with a single imperfection $\delta\hat{\sigma}_i^z$, acting on a time interval τ_g , the transition matrix elements between unperturbed

eigenstates have a typical value:

$$V_{\text{typ}} \sim |\langle \phi_\beta^{(0)} | \delta \hat{\sigma}_i^z \tau_g | \phi_\alpha^{(0)} \rangle| = \epsilon \left| \sum_{m=1}^N c_\alpha^{(m)} c_\beta^{(m)*} \right| \sim \epsilon / \sqrt{N}. \quad (6)$$

The last estimate for V_{typ} results from the sum of N uncorrelated terms. Since the spacing between quasienergy eigenstates is $\Delta E \sim 1/N$, the threshold for the breaking of perturbation theory can be estimated as

$$V_{\text{typ}} / \Delta E \sim \epsilon_\chi \sqrt{N} \sim 1. \quad (7)$$

The analytical result $\epsilon_\chi \sim 1/\sqrt{N}$ is confirmed by the numerical data in Fig.3. The same theoretical argument gives an exponential drop of ϵ_χ for the static imperfection model (3). In this case, the estimate can be obtained with $\delta \rightarrow \delta \sqrt{n_q}$ (sum of n_q random detunings δ_i) and $\tau_g \rightarrow \tau_g n_q \sim \tau_g n_q^2$. This gives $\epsilon_\chi \sim N^{-1/2} n_q^{-5/2}$, again in good agreement with the data of Fig.3. For the case $J = \delta$, the threshold ϵ_χ decreases by a factor ≈ 1.5 at $n_q = 9$ with respect to the $J = 0$ case (see Fig.2), since additional qubit couplings are introduced. We note that the hypersensitivity to perturbations has been proposed as a distinctive feature of chaotic dynamics [18]. However, the authors of Ref. [18] considered the effect of a stochastic environment, while we consider a closed Hamiltonian system.

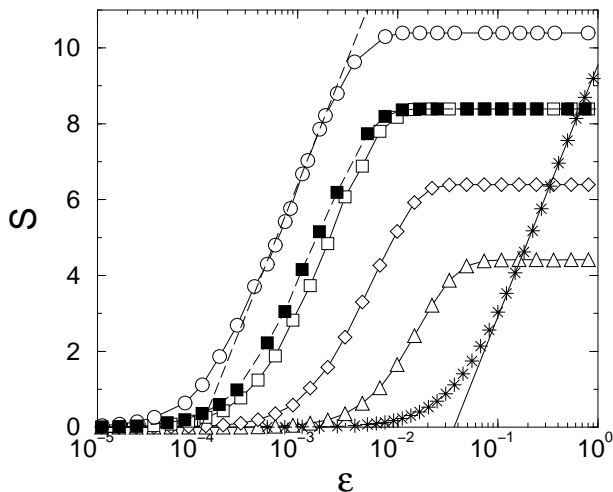


FIG. 2. Quantum eigenstate entropy S as a function of the scaled imperfection strength ϵ for $J = 0$, $n_q = 5$ (triangles), 7 (diamonds), 9 (empty squares), and 11 (circles), for $J = \delta$, $n_q = 9$ (filled squares), and for the single imperfection model at $n_q = 11$ (stars). The straight lines give the theoretical estimates $2^S = A\epsilon^2 N$ (solid line) and $2^S = B\epsilon^2 n_q^5 N$ (taken at $n_q = 11$, dashed line), with the numerically determined constants $A = 0.37$ and $B = 0.25$.

In the mixing regime ($\epsilon > \epsilon_\chi$) the number M of unperturbed eigenfunctions $\phi_\beta^{(0)}$, which have a significant projection over a given $\phi_\alpha^{(\epsilon)}$, is exponentially large. For the

single imperfection model one has $M \sim 2^S \sim \Gamma / \Delta E \sim \epsilon^2 N$, since the mixing takes place inside a Breit-Wigner width given by the Fermi golden rule: $\Gamma \sim V_{\text{typ}}^2 / \Delta E \sim \epsilon^2$. The above estimate for M is in agreement with the numerical data of Fig.2 and is similar to that one used in [8,19] for onset of quantum chaos in the static model (3). We emphasize that this estimate implies that the quantum eigenstate entropy grows linearly with the number of qubits n_q . In the Fermi golden rule regime, the lifetime (measured in number of kicks) of an unperturbed eigenfunction is given by $\tau_\chi \sim 1/\Gamma \propto 1/\epsilon^2$ [8,19]. If the imperfections are described by the model (3), one has $\tau_\chi \sim 1/(\epsilon^2 n_q^5)$. Therefore a reliable quantum computing of the dynamical evolution of the model (2) is possible up to a time scale which drops only *algebraically* with

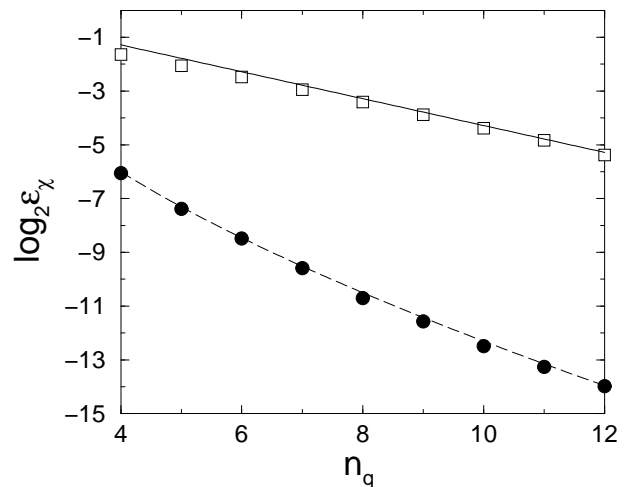


FIG. 3. Dependence of the coupling ϵ_χ at which $S = 1$ on the number of qubits, for $J = 0$ (circles) and for the single imperfection model (squares). The lines give the theoretical dependences $\epsilon_\chi = A^{-1/2} N^{-1/2}$ (above) and $\epsilon_\chi = B^{-1/2} N^{-1/2} n_q^{-5/2}$ (below), with the constants A and B obtained from the data of Fig.2.

the number of qubits, in agreement with the findings of Ref. [7]. In Fig.4 we show the fidelity of quantum evolution, $f(t) = |\langle \psi^{(0)}(t) | \psi^{(\epsilon)}(t) \rangle|^2$. In the top figures, the initial state is an unperturbed eigenstate. For $\epsilon < \epsilon_\chi$ ($S < 1$), the fidelity is very close to 1 at all times, since the eigenstates are not mixed by the imperfections (see Fig.4(a)). On the contrary, in the Fermi golden rule regime $\epsilon \gg \epsilon_\chi$ a perturbed eigenstate, when decomposed into the unperturbed eigenstates, contains a large number of components ($S \gg 1$). The distribution of these components over energy, called local density of states, has a typical Breit-Wigner shape of width Γ . Since its Fourier transform drives the fidelity decay [8,19], one obtains $f(t) \approx \exp(-\Gamma t)$, in agreement with the data of Fig.4(b). The exponential decay continues up to a value $f \approx 1/2^S$ given by the inverse of the number of levels mixed inside the Breit-Wigner width. The case in which the initial wave function $\psi(0)$ is a momentum eigenstate

is considered in Fig.4(c,d). In this case $\psi(0)$ projects significantly over order N unperturbed eigenfunctions. Therefore, for $\epsilon < \epsilon_\chi$, $f(t)$ displays a Gaussian decay (see Fig.4(c), and also Ref. [7]): in this regime the imperfections do not change significantly the eigenstates ($S < 1$), but the initial state is composed of many eigenstates and a Gaussian decay of $f(t)$ is expected from perturbation theory [20,21]. Fig.4(d) shows that in the Fermi golden rule regime ($\epsilon > \epsilon_\chi$) the fidelity decays exponentially, with rate Γ given by the Breit-Wigner width [21]. The decays stops when $f \approx 1/N$, namely when f approaches the inverse of the dimension of the Hilbert space.

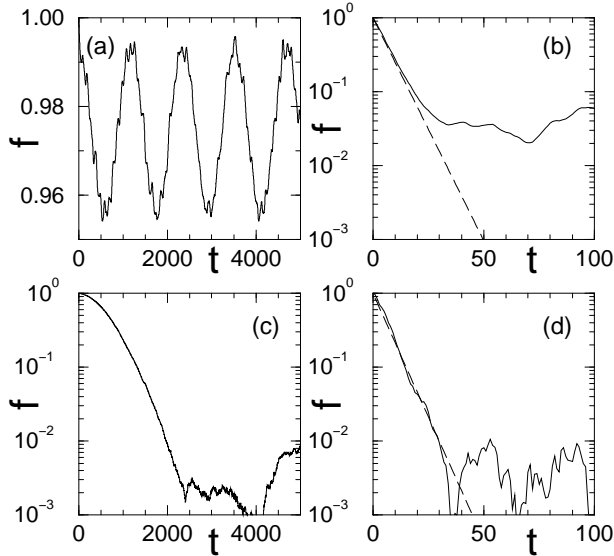


FIG. 4. Fidelity as a function of time, for $n_q = 9$ qubits, $J = 0$, $\epsilon = 10^{-4}$ (left) and $\epsilon = 3 \times 10^{-3}$ (right), with initial wave function a Floquet eigenstate at $\epsilon = 0$ (top) or a momentum eigenstate (bottom). The dashed lines show the exponential decay $f(t) = \exp(-t/t_f)$, with $t_f \approx 7$.

In summary, we have shown that the eigenstates of a quantum computer simulating a system with quantum chaos are hypersensitive to static imperfections: they are significantly different from the exact eigenfunctions above an imperfection strength threshold which drops exponentially with the number of qubits. This border is directly relevant for quantum algorithms which aim at computing static properties of physical systems, for example energy eigenvalues and eigenvectors [22]. We also note that quantum adiabatic algorithms [23] assume the ability to drive the evolution of a quantum state towards the ground state of a specified Hamiltonian. Moreover, a few relevant quantum algorithms can be formulated in terms of determining the eigenvalues corresponding to eigenstates of a given unitary operator [24,25]. Further investigations are required to establish under which conditions the observed hypersensitivity of eigenstates to perturbations could be relevant for the stability of these algorithms.

This work was supported in part by the EC RTN contract HPRN-CT-2000-0156, the NSF under grant No. PHY99-07949 and (for D.L.S.) by the NSA and ARDA under ARO contract No. DAAD19-01-1-0553. Support from the PA INFM “Quantum transport and classical chaos” is gratefully acknowledged.

-
- [1] R.P. Feynman, *Int. J. Theor. Phys.* **21**, 467 (1982).
 - [2] P.W. Shor, in *Proceedings of the 35th Annual Symposium on Foundations of Computer Science*, edited by S. Goldwasser (IEEE Computer Society, Los Alamitos, CA, 1994), p. 124.
 - [3] S.Lloyd, *Science* **273**, 1073 (1996).
 - [4] A. Sørensen and K. Mølmer, *Phys. Rev. Lett.* **83**, 2274 (1999).
 - [5] R. Schack, *Phys. Rev. A* **57**, 1634 (1998).
 - [6] B. Georgeot and D.L. Shepelyansky, *Phys. Rev. Lett.* **86**, 2890 (2001); **86**, 5393 (2001).
 - [7] G. Benenti, G. Casati, S. Montangero, and D.L. Shepelyansky, *Phys. Rev. Lett.* **87**, 227901 (2001).
 - [8] B. Georgeot and D.L. Shepelyansky, *Phys. Rev. E* **62**, 3504 (2000); **62**, 6366 (2000); G. Benenti, G. Casati, and D.L. Shepelyansky, *Eur. Phys. J. D* **17**, 265 (2001).
 - [9] C. Miquel, J.P. Paz, and R. Perazzo, *Phys. Rev. A* **54**, 2605 (1996).
 - [10] J.I. Cirac and P. Zoller, *Phys. Rev. Lett.* **74**, 4091 (1995).
 - [11] C. Miquel, J.P. Paz, and W.H. Zurek, *Phys. Rev. Lett.* **78**, 3971 (1997).
 - [12] P.H. Song and D.L. Shepelyansky, *Phys. Rev. Lett.* **86**, 2162 (2001).
 - [13] O.P. Sushkov and V.V. Flambaum, *Sov. Phys. Usp.* **25**, 1 (1982).
 - [14] See, e.g., A. Ekert and R. Jozsa, *Rev. Mod. Phys.* **68**, 733 (1996).
 - [15] See, e.g., N.A. Gershenfeld and I.L. Chuang, *Science* **275**, 350 (1997).
 - [16] The computation of Husimi functions is described in S.-J. Chang and K.-J. Shi, *Phys. Rev. A* **34**, 7 (1986).
 - [17] In order to stress the perturbation induced symmetry breaking, in Fig.1 we consider the time-symmetric version of the map (2): $\bar{\psi} = \hat{U}\psi = e^{-iT\hat{n}^2/4} e^{ik(\hat{\theta}-\pi)^2/2} e^{-iT\hat{n}^2/4} \psi$. This map has axial symmetry contrary to central symmetry for map (2).
 - [18] R. Schack and C.M. Caves, *Phys. Rev. Lett* **71**, 525 (1993); *Phys. Rev. E* **53**, 3257 (1996).
 - [19] V.V. Flambaum, *Aust. J. Phys.* **53**, 489 (2000).
 - [20] N.R. Cerruti and S. Tomsovic, nlin.CD/0108016.
 - [21] Ph. Jacquod, P.G. Silvestrov, and C.W.J. Beenakker, *Phys. Rev. E* **64**, 055203(R) (2001).
 - [22] D.S. Abrams and S. Lloyd, *Phys. Rev. Lett.* **83**, 5162 (1999).
 - [23] E. Farhi, J. Goldstone, S. Gutmann, J. Lapan, A. Lundgren, and D. Preda, *Science* **292**, 472 (2001).
 - [24] A.Yu. Kitaev, quant-ph/9511026.
 - [25] R. Cleve, A.Ekert, C.Macchiavello, and M. Mosca, *Proc. R. Soc. London A* **454**, 339 (1998).